

Anti-diabetic Activity of a Polyphenol-rich Extract from *Phellinus igniarius* in KK-Ay Mice with Spontaneous Type 2 Diabetes Mellitus

Sijian Zheng^{a,1}, Shihao Deng^{a,1}, Yun Huang^a, Mi Huang^a, Ping Zhao^b, Xinhua Ma^a,
Yanzhang Wen^a, Qiang Wang^{a,*}, Xinzhou Yang^{a,c,*}

^aSchool of Pharmaceutical Sciences, South-Central University for Nationalities, 182 Min-Zu Road, Wuhan 430074, China

*E-mail addresses: wq@mail.scuec.edu.cn (Q. Wang); xzyang@mail.scuec.edu.cn (X.Z. Yang); Fax: +86 27 67841196; Tel.: +86 27 67841196.

^bSchool of Life Sciences, South-Central University for Nationalities, 182 Min-Zu Road, Wuhan 430074, China

^cNational Demonstration Center for Experimental Ethnopharmacology Education, South-Central University for Nationalities, 182 Min-Zu Road, Wuhan 430074, China

¹Both authors contributed equally to this paper.

Supporting Information Contents:

S1. Screening methodology validation

S2. HPLC chromatogram of PI-PRE at 220, 254, 320 nm

S3. Determination of total polyphenol content of PI-PRE

S4. GLUT4 translocation assay of compounds from PI-PRE in L6 cells

S5. Glucose uptake test of compounds from PI-PRE in L6 cells

S6. ¹H-NMR spectrum of Compound 1

S7. ¹³C-NMR spectrum of Compound 1

S8. ESIMS spectrum of Compound 1

S9. ¹H-NMR spectrum of Compound 2

S10. ¹³C-NMR spectrum of Compound 2

S11. ESIMS spectrum of Compound 2

S12. ¹H-NMR spectrum of Compound 3

S13. ¹³C-NMR spectrum of Compound 3

S14. ESIMS spectrum of Compound 3

S15. ¹H-NMR spectrum of Compound 4

S16. ¹³C-NMR spectrum of Compound 4

S17. ESIMS spectrum of Compound 4

S1. Screening Methodology Validation

There are several papers reported that IRAP-mOrange and GLUT4-eGFP could be applied to detect the GLUT4 translocation in L6 (Wang et al., 2009; Zhou et al., 2016; Huang et al., 2016) and 3T3-L1 cells (Bai et al., 2007; Jiang et al. 2008). In order to validate the feasibility of our IRAP translocation assay for discovering potential hypoglycemic agents, we have observed the effects when the GLUT4-eGFP or IRAP-marked L6 cells treated with insulin and berberine which are definitely pharmacodynamic GLUT4 agonists. L6 cells which stably express IRAP-mOrange and GLUT4-eGFP were cultured in MEM- α supplemented with 10% fetal bovine serum and 1% antibiotics (100 U/mL penicillin and 100 μ g/mL streptomycin) at 37 °C in 5% CO₂. L6 cells was seeded in 48 well plates, and incubated until 100% confluence and then starved in serum-free MEM- α for 2 h. Afterwards, L6 cells were treated with insulin (10 nM) and berberine (5 μ M). The cells were taken photos with a laser-scanning confocal microscope LSM 510 (Carl Zeiss, Jena, Germany) to supervise the IRAP-mOrange and GLUT4-eGFP translocation. And the images were captured with 555 nm excitation laser every 10 seconds in first 5 minutes and then every 5 minutes in later 30 minutes.

During the experiment, as time went on, we could observe the green and red fluorescence enhanced significantly after treating with insulin and berberine in L6 cells (Fig. S1). The results showed that GLUT4 and IRAP simultaneously translocated onto the plasma membrane in 30 min when adding the GLUT4 agonist. GLUT4 has mainly been recruited to the PM throughout to the GLUTs storage vesicles (GSV). Three main proteins stored in GSV are GLUT4, IRAP, and Sortilin (Shi et al., 2005). It was reported that IRAP

and GLUT4 displayed a strong colocalization (Kumar et al., 2010; Rubin et al., 2009) in many researches. Thus, detecting the IRAP can indirectly reflect the situation of GLUT4. So our results could be explained that detecting the IRAP-mOrange fluorescence could indirectly reflect the GLUT4 translocation. As the red fluorescence is more conspicuous than green fluorescence for observation, so we choose the IRAP-mOrange fluorescence assay for reflecting GLUT4 translocation.

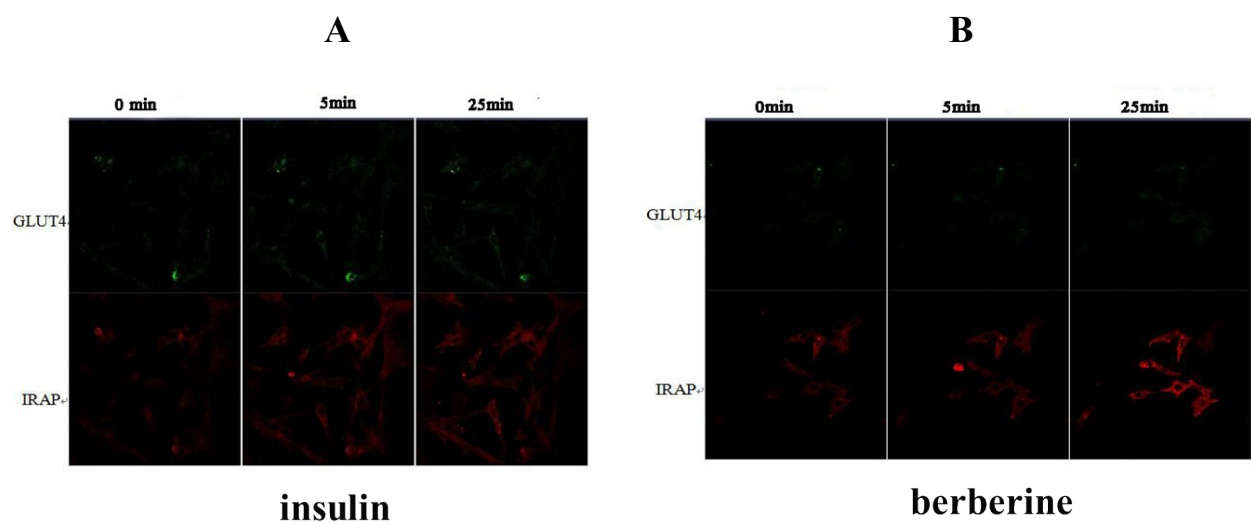


Figure S1 L6 cells were infected with IRAP-mOrange and GLUT4-eGFP in order to detect externalized GLUT4 translocation by confocal microscopy. (A) Confocal images in L6 cells incubated in the absence (0 min) or presence of insulin for 5min, 30 minutes. (B) Confocal images in L6 cells incubated in the absence (0 min) or presence of berberine for 5 min, 30 minutes.

References

- Bai, L., Wang, Y., Fan, J., et al. (2007). Dissecting multiple steps of GLUT4 trafficking and identifying the sites of insulin action. *Cell Metab.* 5, 47-57.
- Huang, M., Zhao, P., Xiong, M. R., et al. (2016). Antidiabetic activity of

- perylenequinonoid-rich extract from *Shiraia bambusicola* in KK-Ay Mice with Spontaneous Type 2 Diabetes Mellitus. *J. Ethnopharmac.* 191, 71-81.
- Jiang, L., Fan, J., Bai, L., et al. (2008). Direct quantification of fusion rate reveals a distal role for AS160 in insulin-stimulated fusion of GLUT4 storage vesicles. *J. Biol. Chem.* 283, 8508-8516.
- Kumar, A., Lawrence, Jr., Jung, D. Y., et al. (2010). Fat cellspecific ablation of rictor in mice impairs insulin-regulated fat cell and whole-body glucose and lipidmetabolism. *Diabetes.* 59, 1397–1406. doi: 10.2337/db09-1061.
- Nishiumi, S., Ashida, H. (2007). Rapid preparation of a plasma membrane fraction from adipocytes and muscle cells: application to detection of translocated glucose transporter 4 on the plasma membrane. *Biosci. Biotechnol. Biochem.* 71, 2343-2346.
- Rubin, B. R., Bogan, J. S. (2009). Intracellular retention and insulinstimulated mobilization of GLUT4 glucose transporters. *Vitam. Horm.* 80, 155–192. doi: 10.1016/S0083-6729(08)00607-9.
- Shi, J., Kandror, K. V. (2005). Sortilin is essential and sufficient for the formation of glut4 storage vesicles in 3T3-L1 adipocytes. *Dev. Cell.* 9, 99–108.
- Wang, X., Qu, F., Chen, Z., et al. (2009). Labeling and imaging of GLUT4 in live L6 cells with quantum dots. *Biochem. Cell. Biol.* 87, 687-694.
- Zhou, Q., Yang, X. Z., Xiong, M. R., et al. (2016). Chloroquine Increases Glucose Uptake via Enhancing GLUT4 Translocation and Fusion with the Plasma Membrane in L6 Cells. *Cell Physiol. Biochem.* 38, 2030-2040.

S2. HPLC chromatogram of PI-PRE at 220, 254, 320 nm

Analysis was carried out on a Waters Sunfire C₁₈ column (5 μ m, 4.6 \times 150 mm i.d.) equipped with a Waters Sunfire C₁₈ cartridge as a precolumn. Acetonitrile in water with 0.1 % formic acid from 10 to 100 %, 25 min, 100% acetonitrile holding for the next 5 min. The analysis was performed at the flow rate of 1.0 mL/min. UV-Vis spectra were recorded with the range of 200-500 nm at a spectral acquisition rate of 10 scans per second. Finally, we chose 220, 254, 320 nm (Fig. S2, S3, S4) to calculate the integration and ratio of each peak area respectively. The integration of peaks and ratio of peak area were listed in Table 1. According to HPLC data (Table S1), the total percentage of four peaks at 220, 254, and 320 nm were 93.73 %, 85.51 %, and 89.52 % respectively, which suggest that the percentage yields of the 4 phenols in PI-PRE was more than 85%.

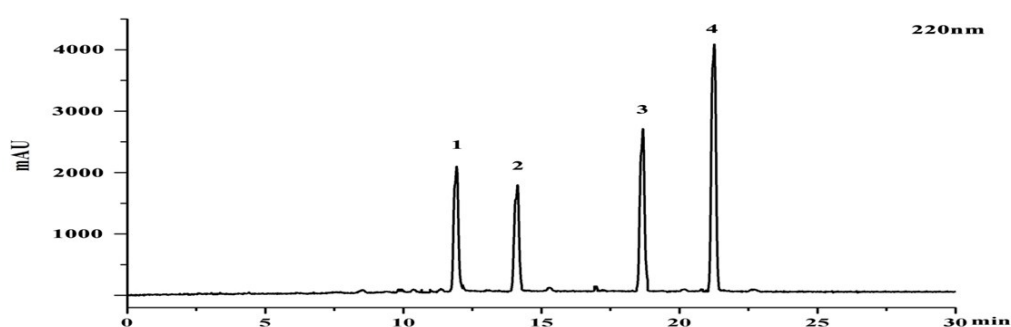


Figure S2 The HPLC chromatogram of PI-PRE at 220 nm

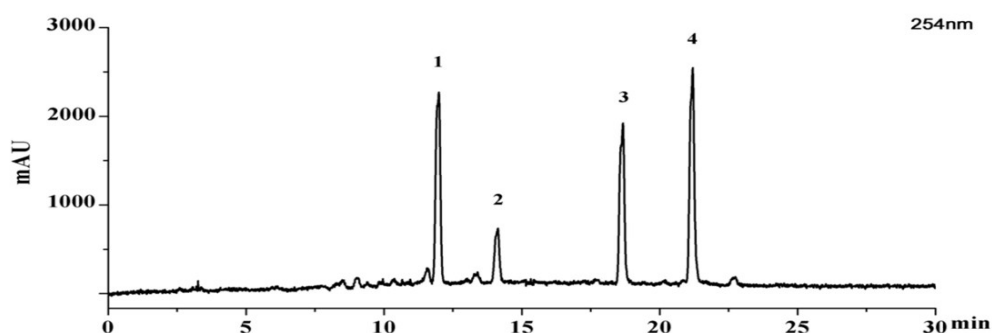


Figure S3 The HPLC chromatogram of PI-PRE at 254 nm

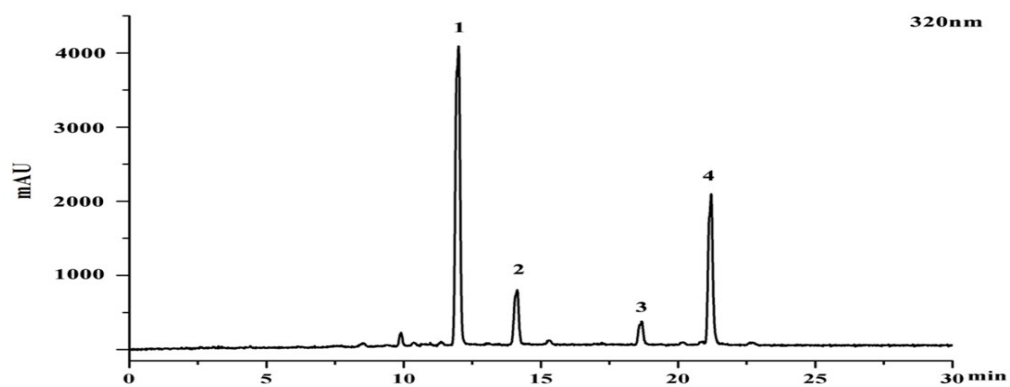


Figure S4 The HPLC chromatogram of PI-PRE at 320 nm

Table S1 The integration of peaks and ratio of peak area at 220, 254, 320 nm

Compound	220 nm		254 nm		320 nm	
	Peak Area	% Area	Peak Area	% Area	Peak Area	% Area
1	166748	20.80	214553	24.55	459515	51.93
2	157448	19.64	46656	5.34	71506	8.08
3	192561	24.02	195666	22.39	37469	4.23
4	234649	29.27	290417	33.23	223736	25.28
Total	751406	93.73	747292	85.51	792226	89.52

S3. Determination of total polyphenol content of PI-PRE

Total polyphenol content was determined by a modified Folin–Ciocalteu method (Quiñones et al., 2011). 3.0 ml of Folin–Ciocalteu reagent, 6.0 mL of 15% sodium carbonate and 0.40ml of PI-Dichloromethane, 0.12 mL of PI-PRE (1.0 mg mL⁻¹) were mixed in 25 ml glass vial, and the absorbance at 760 nm was measured after 60 minutes at 20°C. As a result, total polyphenol content of PI-Dichloromethane and PI-PRE was 221.8 ± 7.51, and 476.8 ± 10.97 mg/g (gallic acid equivalents), respectively.

Table S2 Total polyphenol content in PI-Dichloromethane and PI-PRE

Total polyphenol content	mg /g
PI-Dichloromethane	221.8 ± 7.51
PI-PRE	476.8 ± 10.97

*The values are expressed as the mean ± SEM (n = 3).

References

Quiñones, M., Miguel, M., Muguera, B., et al., A. Effect of a cocoa polyphenol extract in spontaneously hypertensive rats. *Food. Funct.* 2011, 11, 649-653.

S4. GLUT4 translocation assay of compounds from PI-PRE in L6 cells

L6 cells were transfected with pIRAP-mOrange cDNAs using Lipofectamine 2000 according to the manufacturers' protocol. L6 cells stably expressing IRAP-mOrange were incubated with MEM- α supplied with 10% FBS and 1% antibiotics at 37°C in 5% CO₂. Before the experiment, L6 cells were seeded into 24-well plates for 12 h and then starved in serum-free MEM- α containing 2% FBS and 1% antibiotics for 2 h. The cells were viewed with a confocal laser scanning microscope LSM 510 (CarlZeiss, Jena, Germany) to monitor IRAP-mOrange translocation. Images were taken after addition of PI-PRE (10 μ g/mL), compounds 1~4 (10 μ g/mL), Insulin (10 nM) or vehicle control (0.1% DMSO) for 30 min using 555 nm excitation laser.

The results were shown in Figure S5, At a dose of 10 μ g/mL, PI-PRE stimulated GLUT4 translocation by 1.53-fold in L6 cells. Four compounds affected GLUT4 translocation in different degrees, compound 4 (inoscavin C) and compound 3 (7,3'-dihydroxy-5'-methoxyisoflavone) showed stronger effects on promoting GLUT4 translocation by 1.87-fold, 1.62-fold respectively, compared with non-treated cells.

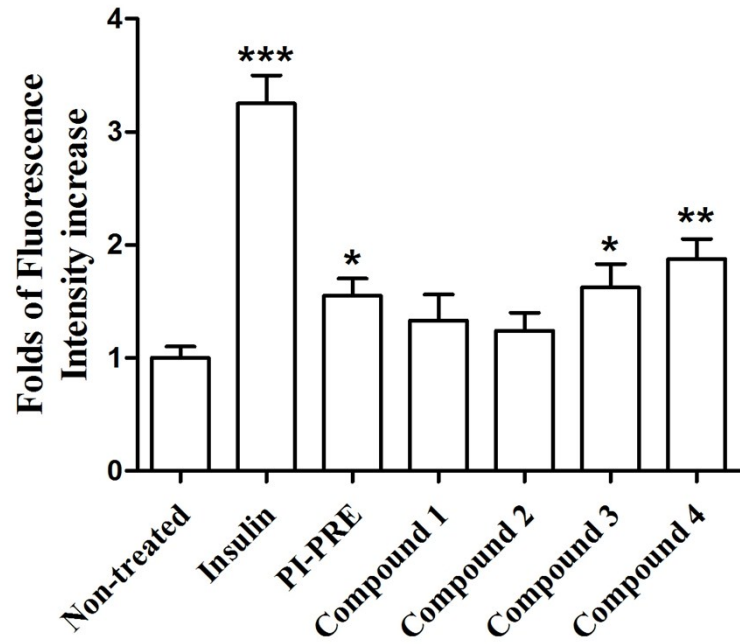


Figure S5 Effects of compounds from PI-PRE on stimulating GLUT4 translocation in L6 cells. Data represent the fold increase in fluorescence induced by different test samples at 30 minutes (* $P < 0.05$, compared with non-treated groups; ** $P < 0.01$, compared with non-treated groups; *** $P < 0.001$, compared with non-treated groups).

S5. Glucose uptake test of compounds from PI-PRE in L6 cells

A cell-based 2-[N-(7-nitrobenz-2-oxa-1,3-dioxol-4-yl)amino]-2-deoxyglucose (2-NBDG) Glucose Uptake Assay Kit (Cayman Chemical, USA) was used to evaluate glucose uptake activity of four separate compounds in PI-PRE in L6 cells. L6 cells were seeded in a 96-well black plate with the density $1 \times 10^4 - 5 \times 10^4$ cells /well in 100 μL α -MEM medium. Subsequently, cells were treated with PI-PRE (10 $\mu\text{g}/\text{mL}$), compounds 1~4 (10 $\mu\text{g}/\text{mL}$), Insulin (10 nM) or vehicle control (0.1% DMSO) in 100 μL glucose-free α -MEM medium containing 150 $\mu\text{g}/\text{mL}$ 2-NBDG. Plates were incubated in culture incubator at 37°C with 5% CO_2 for 24 h. After incubation, plates were centrifuged for 5 min at 400 g at room temperature. The supernatant was aspirated, and 200 μL of cell-based assay buffer was added into each well. This procedure was repeated twice to ensure cells washed up. Then, 100 μL of assay buffer was added into each well. The 2-NBDG taken up by cells was detected with fluorescent microplate reader (excitation/emission= 485/535 nm).

The results were shown in Figure S6, insulin significantly increased glucose uptake by 2.26-fold in L6 cells, as evidenced by the increasing fluorescence intensity compared with the non-treated cells. At a dose of 10 $\mu\text{g}/\text{mL}$, PI-PRE increased glucose uptake by 1.40-fold, four compounds increased glucose uptake in different degrees, compound 4 (inoscavin C) and compound 3 (7,3'-dihydroxy-5'-methoxyisoflavone) showed stronger effects on promoting glucose uptake by 1.68-fold, 1.45-fold respectively, compared with non-treated cells.

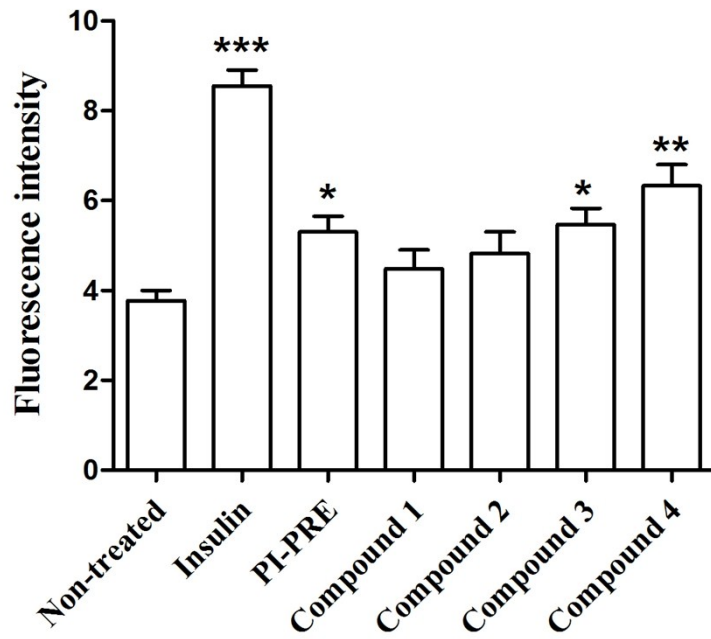
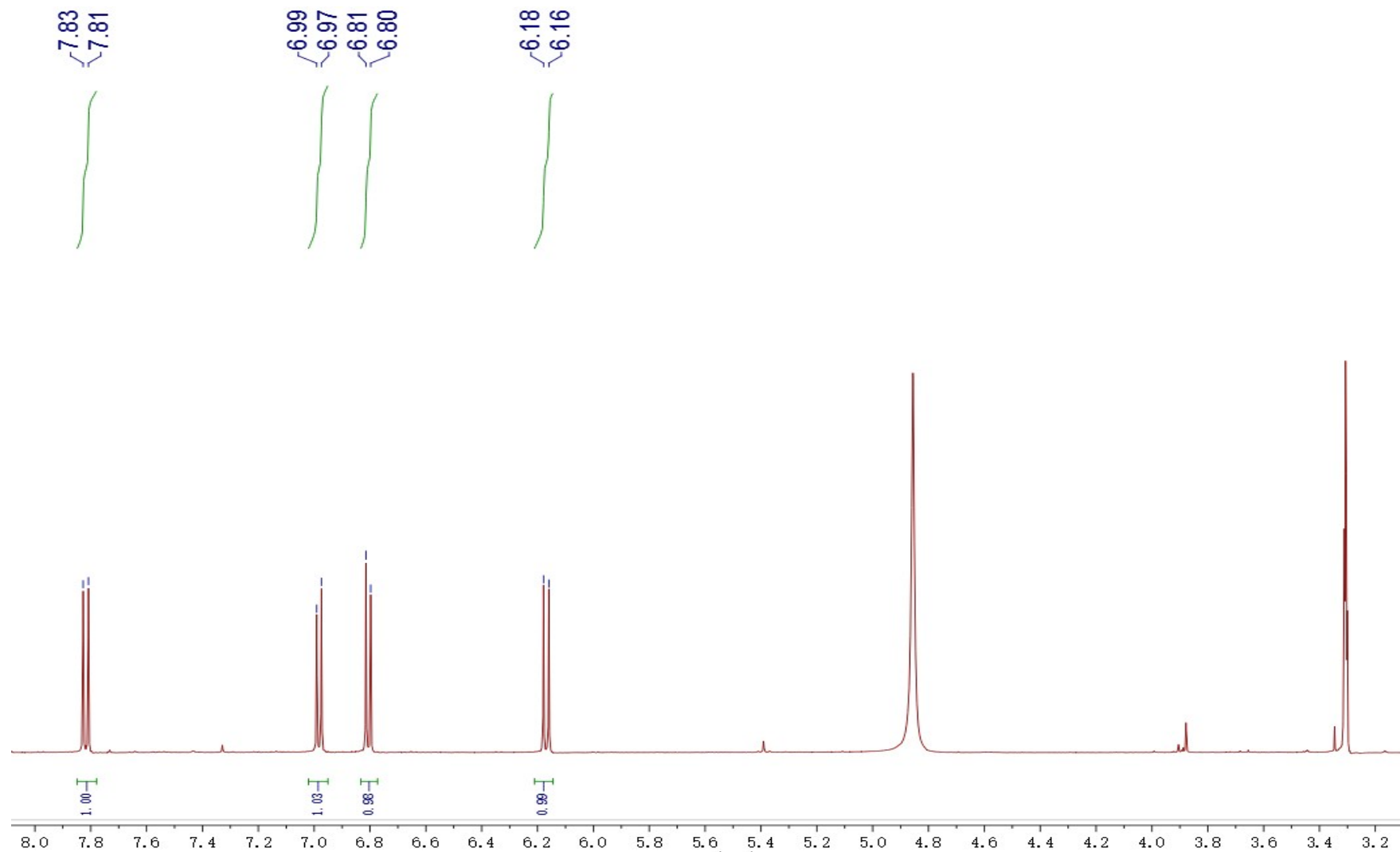
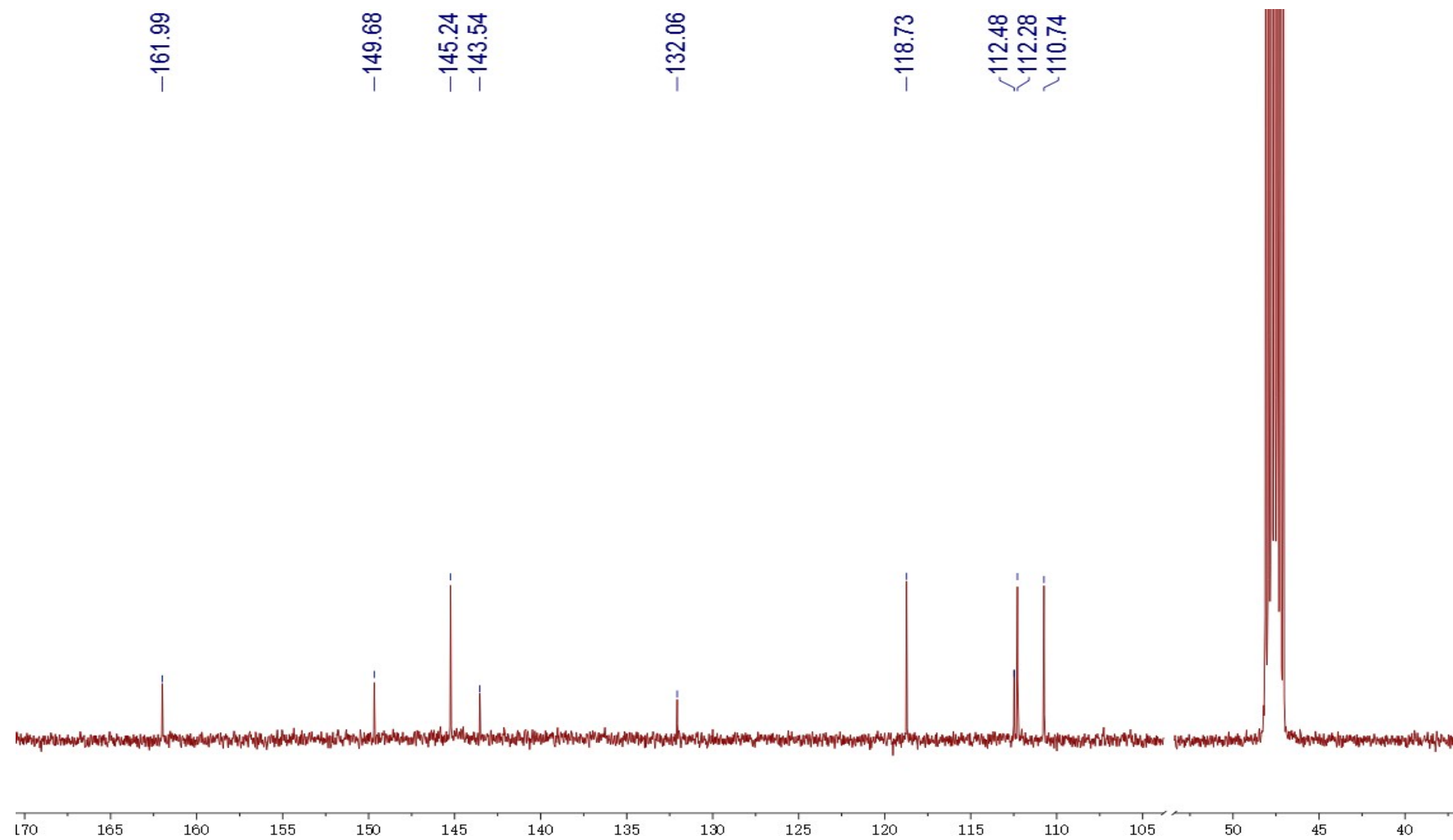


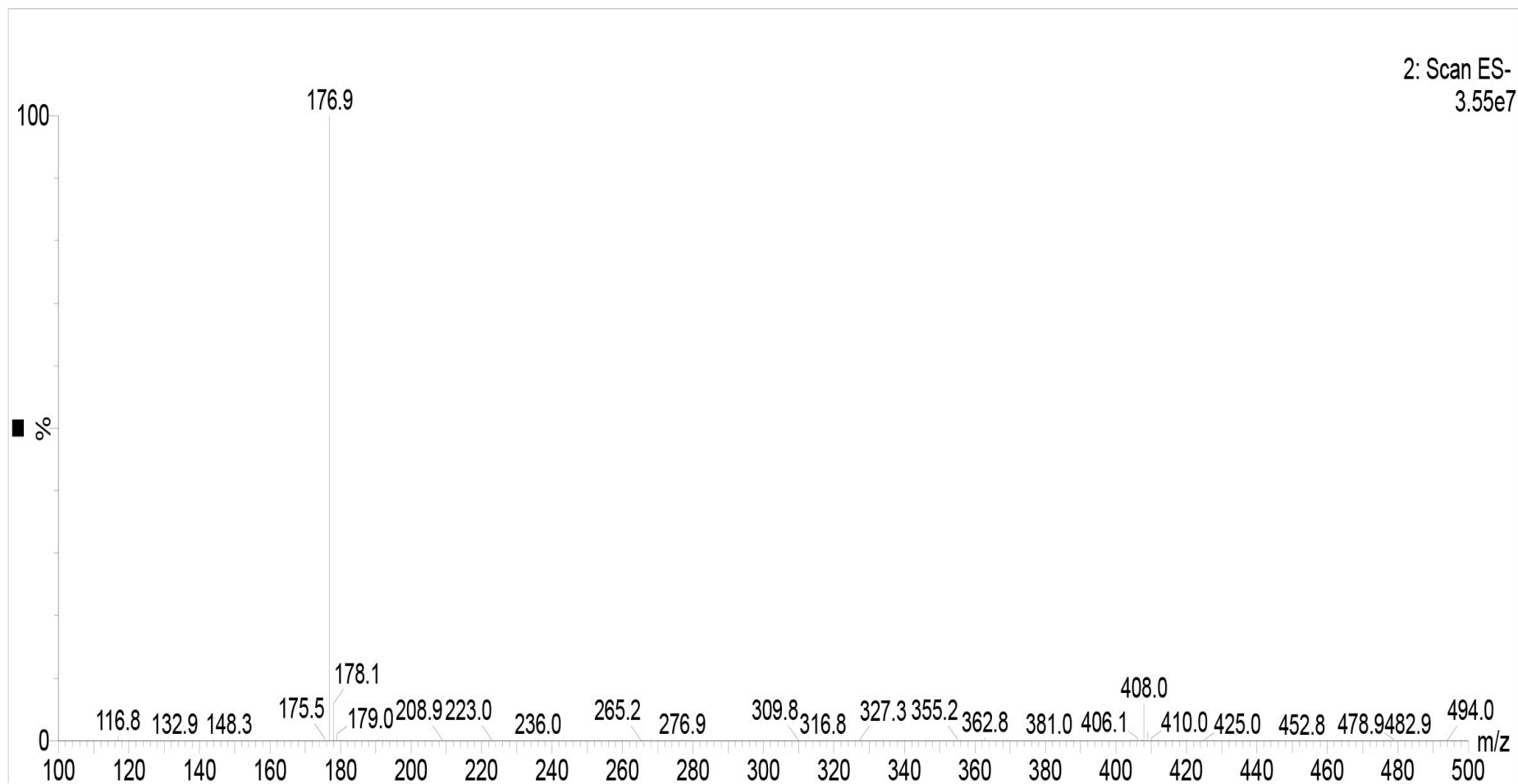
Figure S6 Effects of 4 compounds from PI-PRE on glucose uptake in L6 cells (* $P < 0.05$, compared with non-treated groups; *** $P < 0.001$, compared with non-treated group).



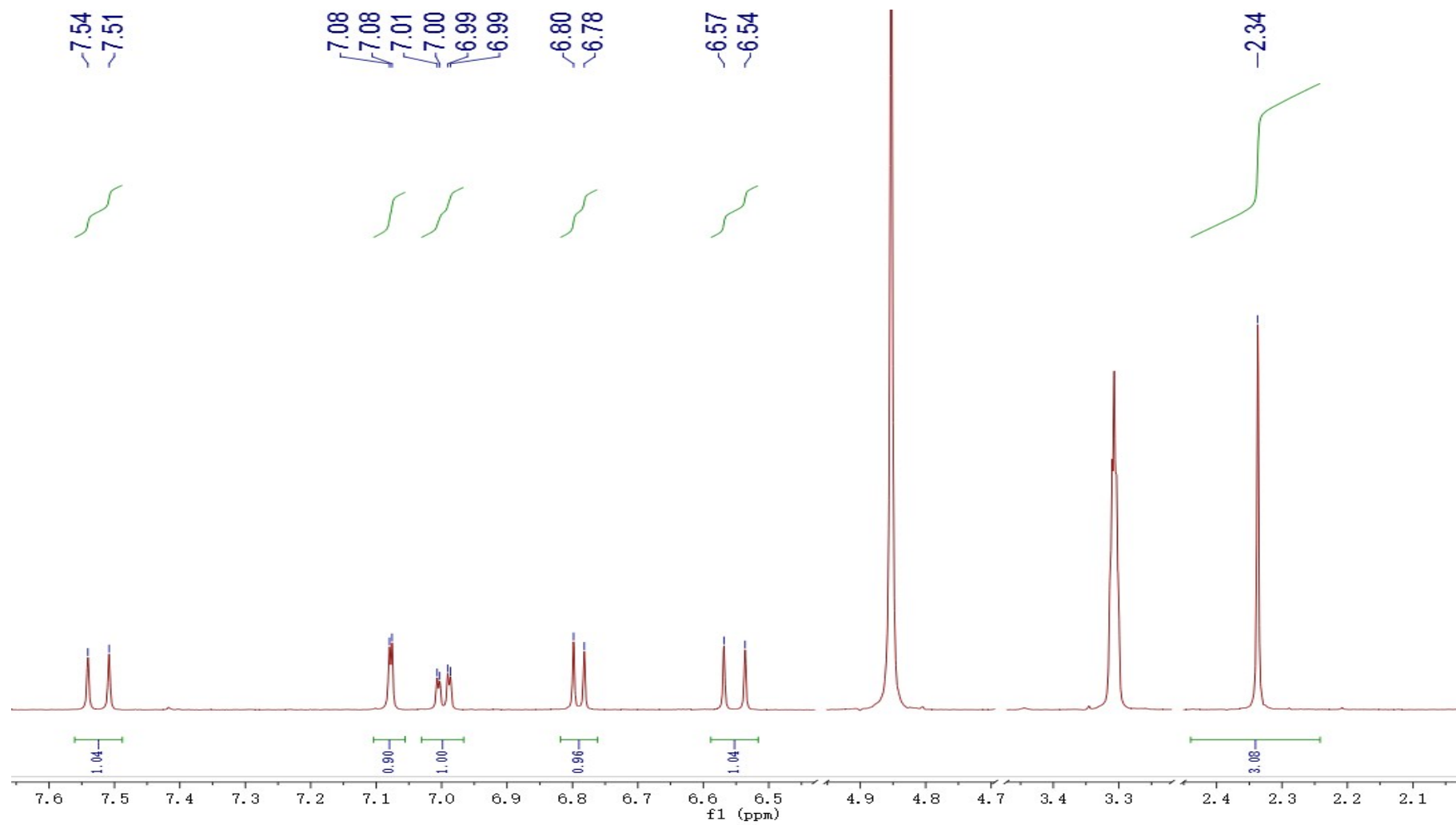
S6. $^1\text{H-NMR}$ spectrum of Compound 1



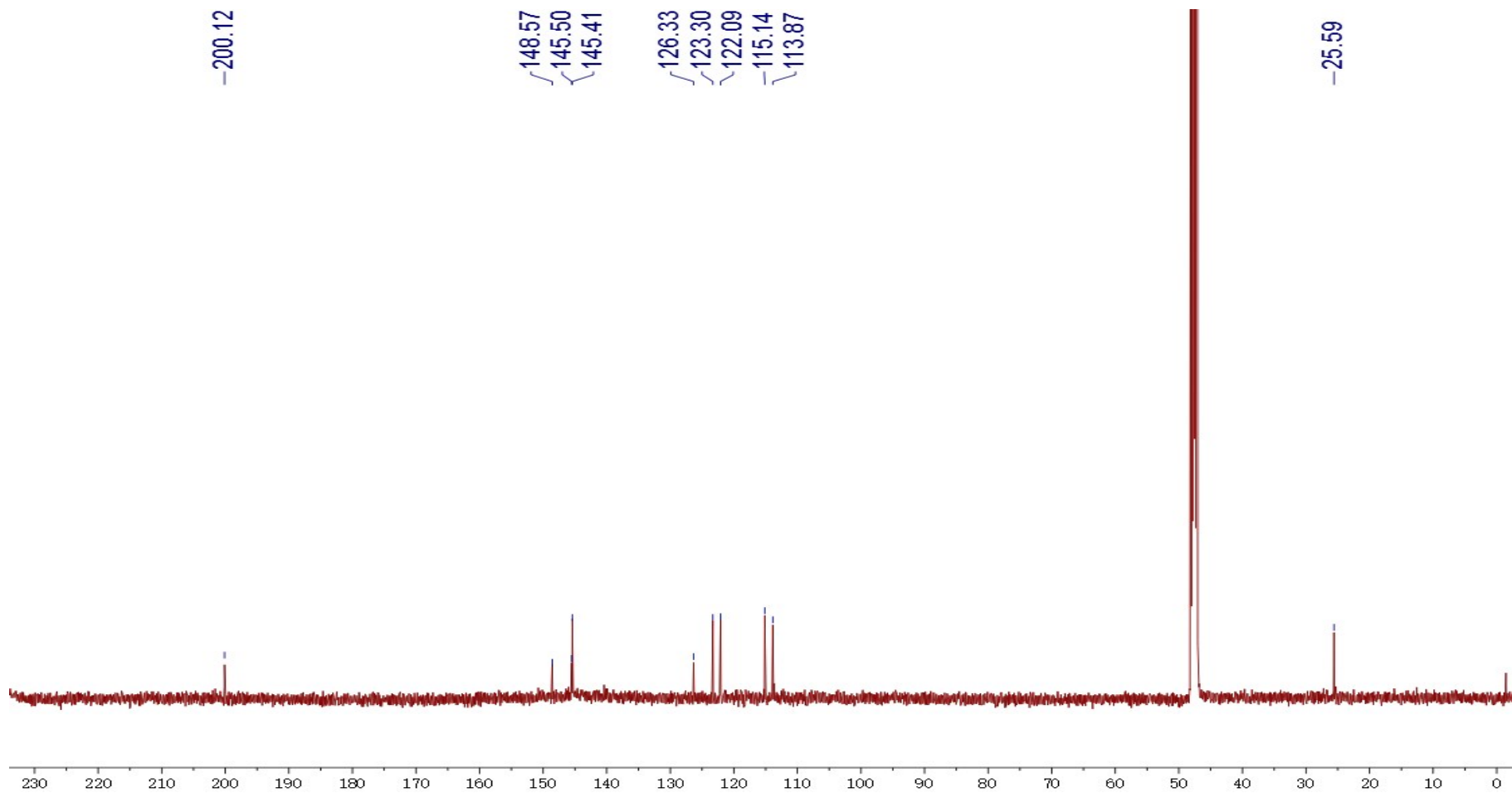
S7. ^{13}C -NMR spectrum of Compound 1



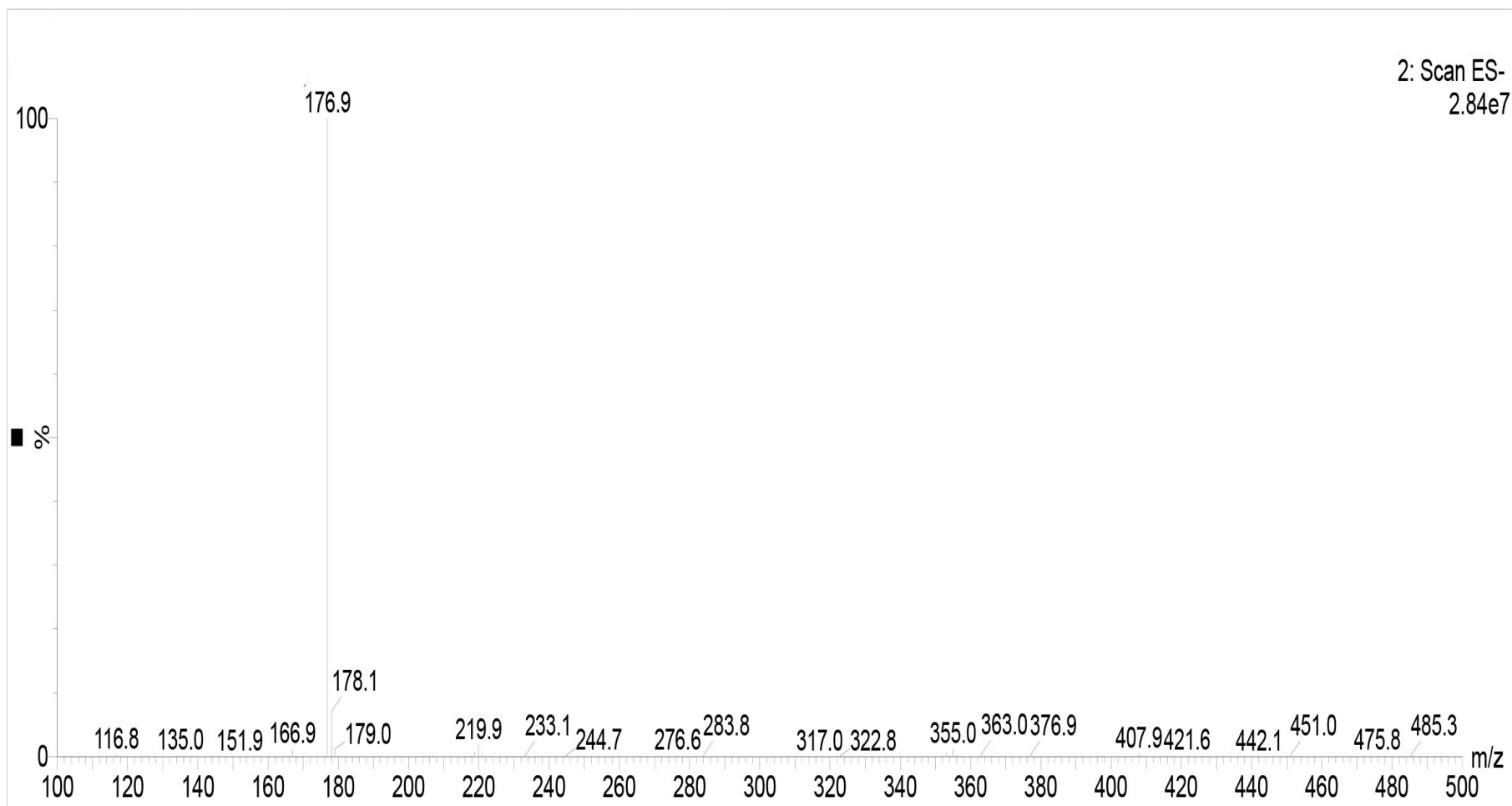
S8. ESIMS spectrum of Compound 1



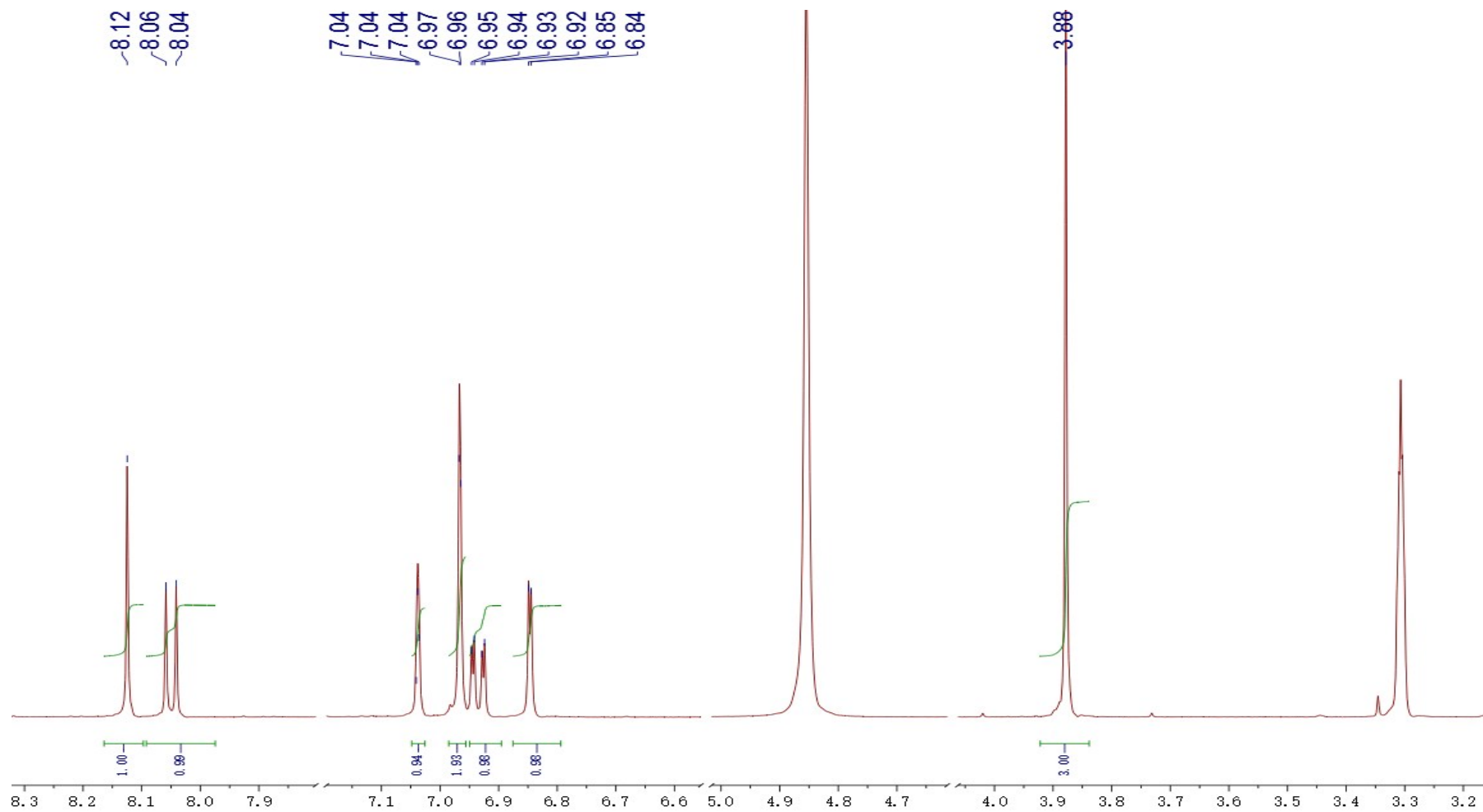
S9. $^1\text{H-NMR}$ spectrum of Compound 2



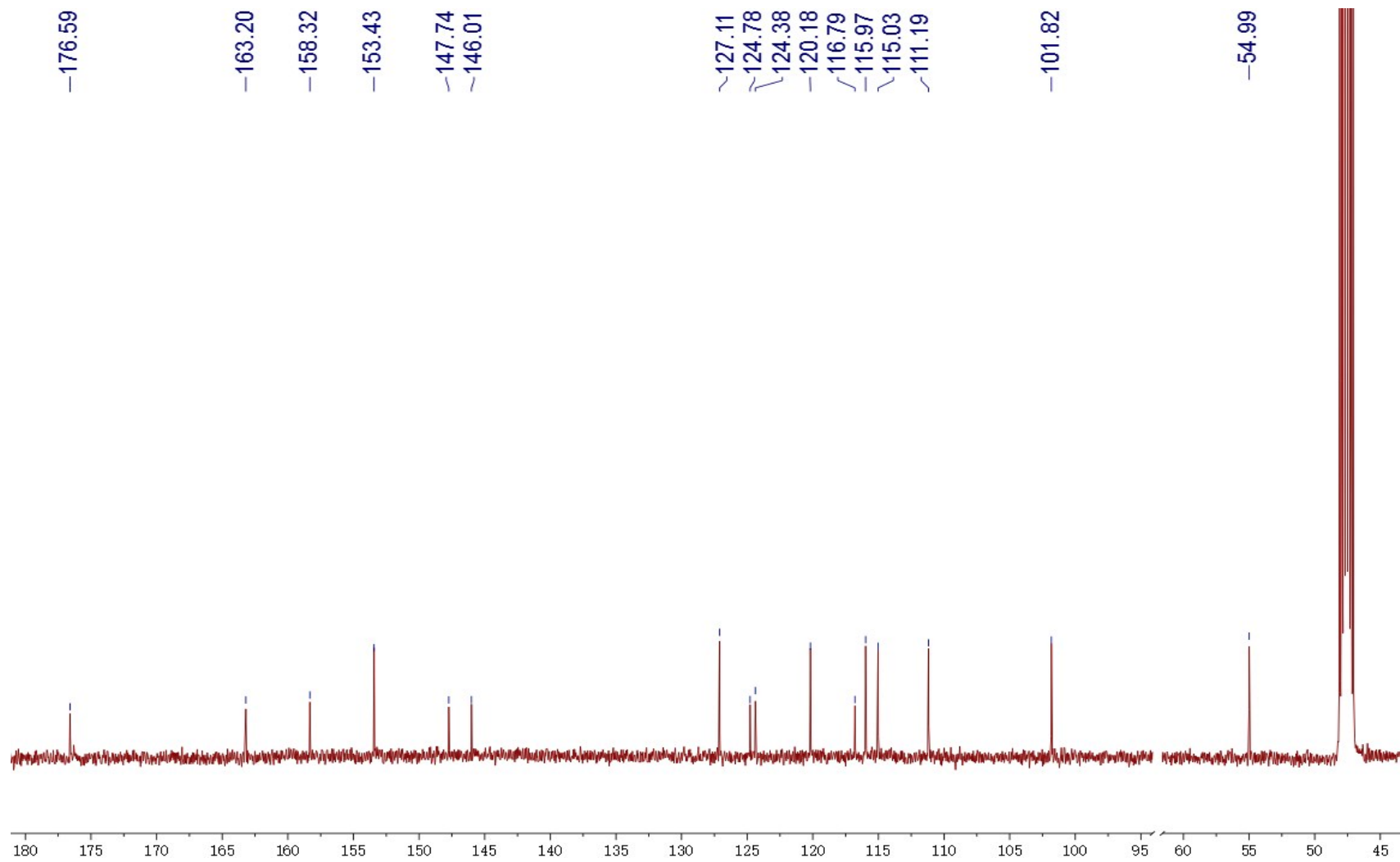
S10. ^{13}C -NMR spectrum of Compound 2



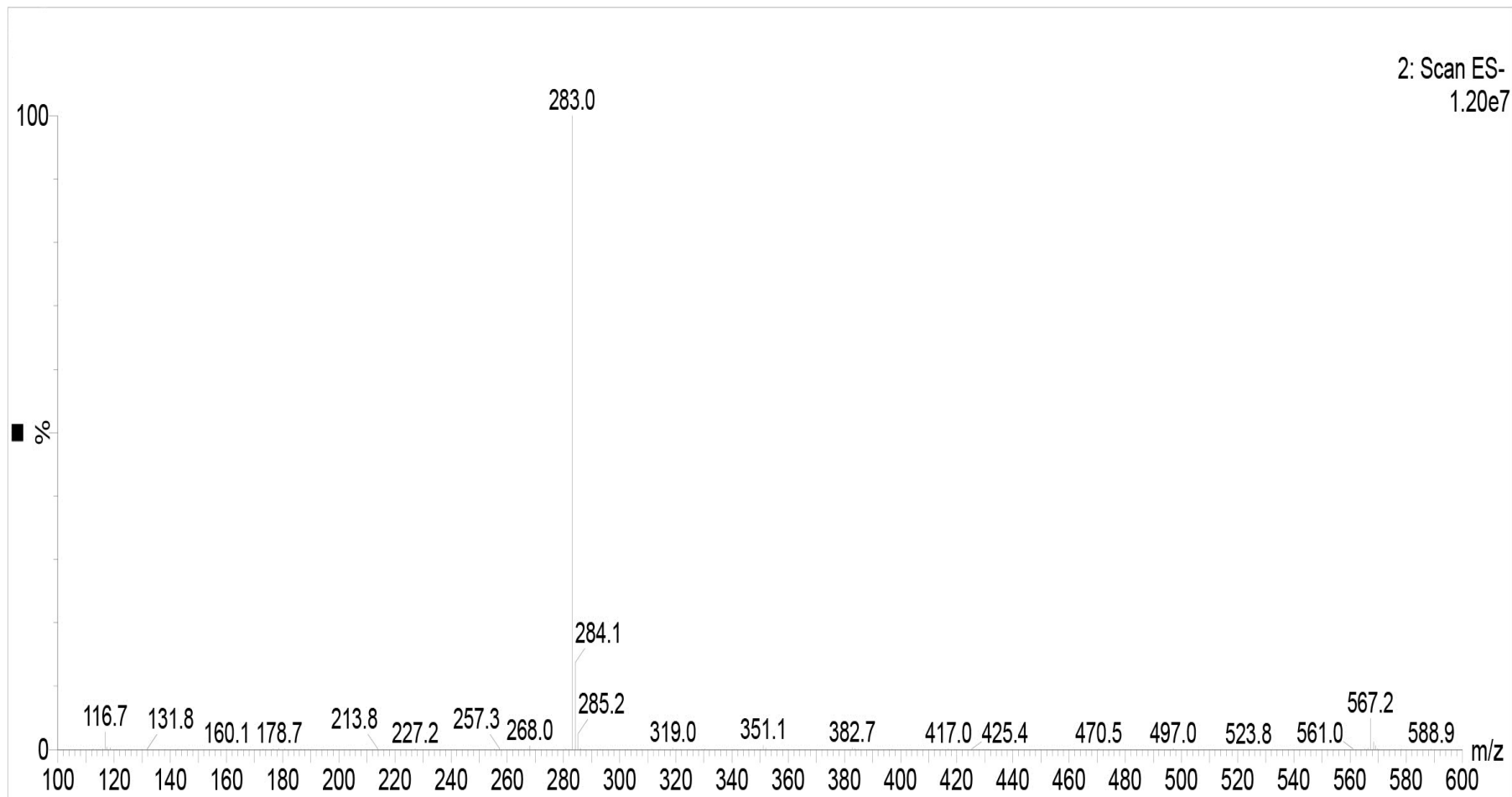
S11. ESIMS spectrum of Compound 2



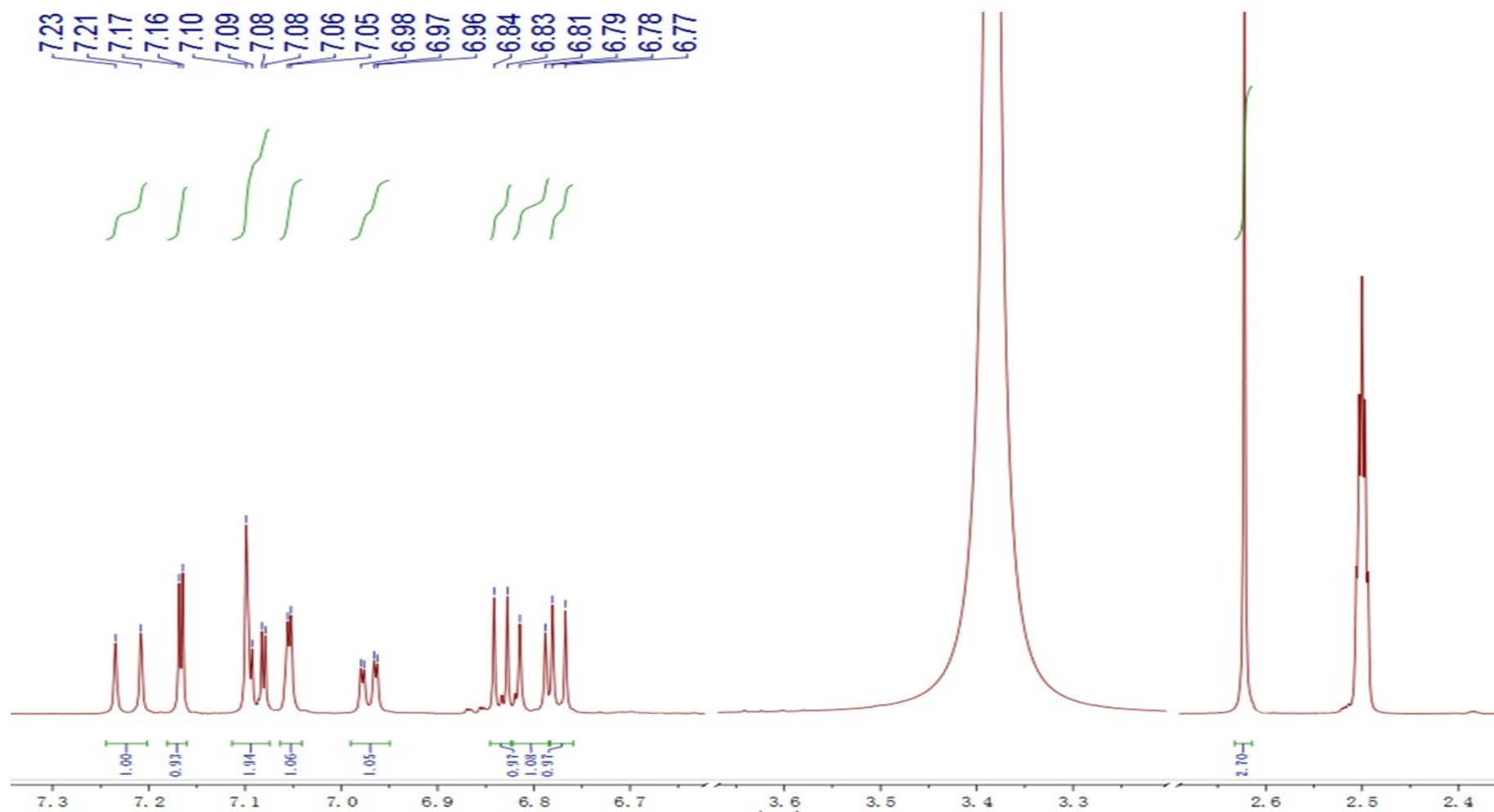
S12. $^1\text{H-NMR}$ spectrum of Compound 3



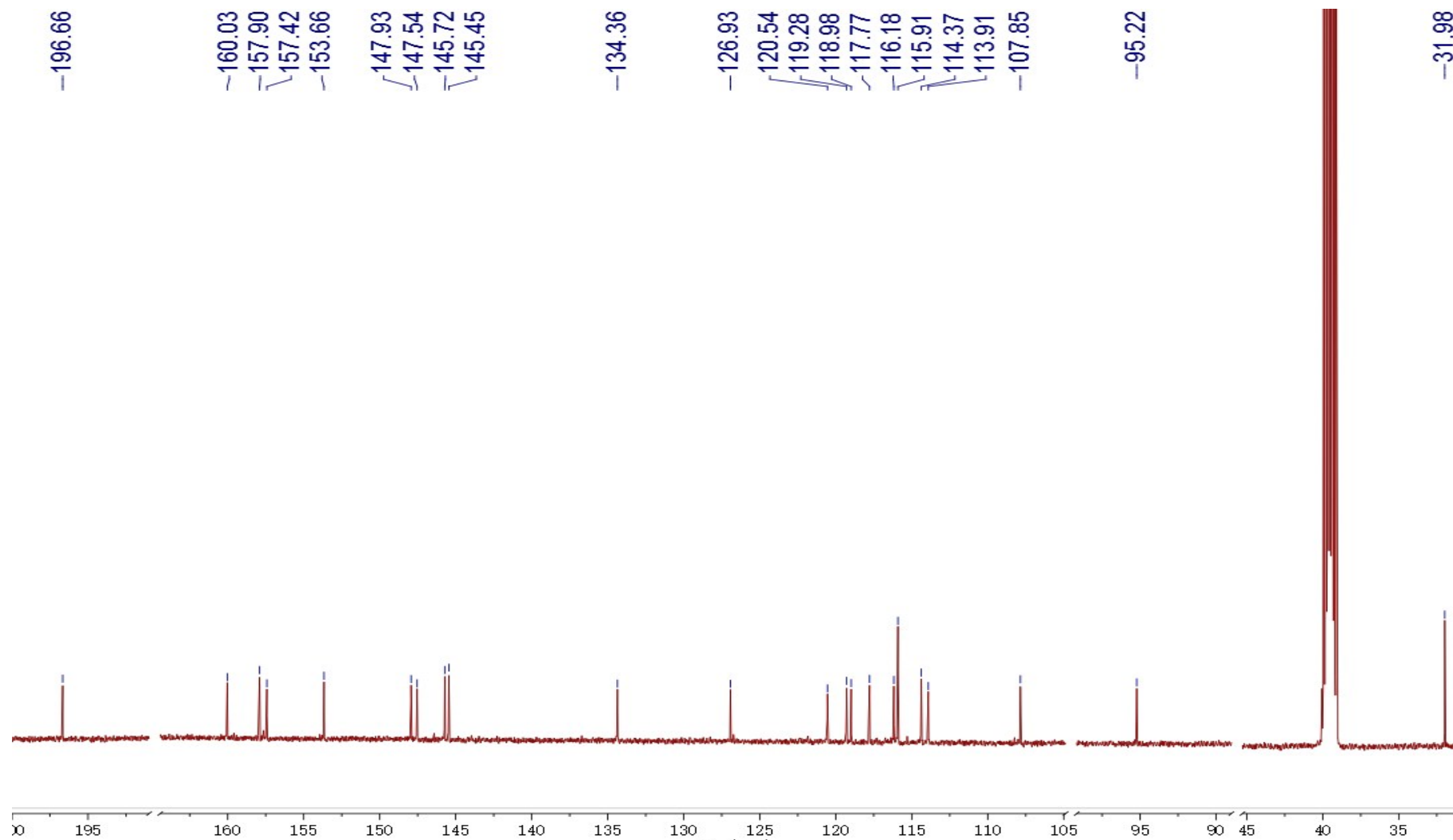
S13. ^{13}C -NMR spectrum of Compound 3



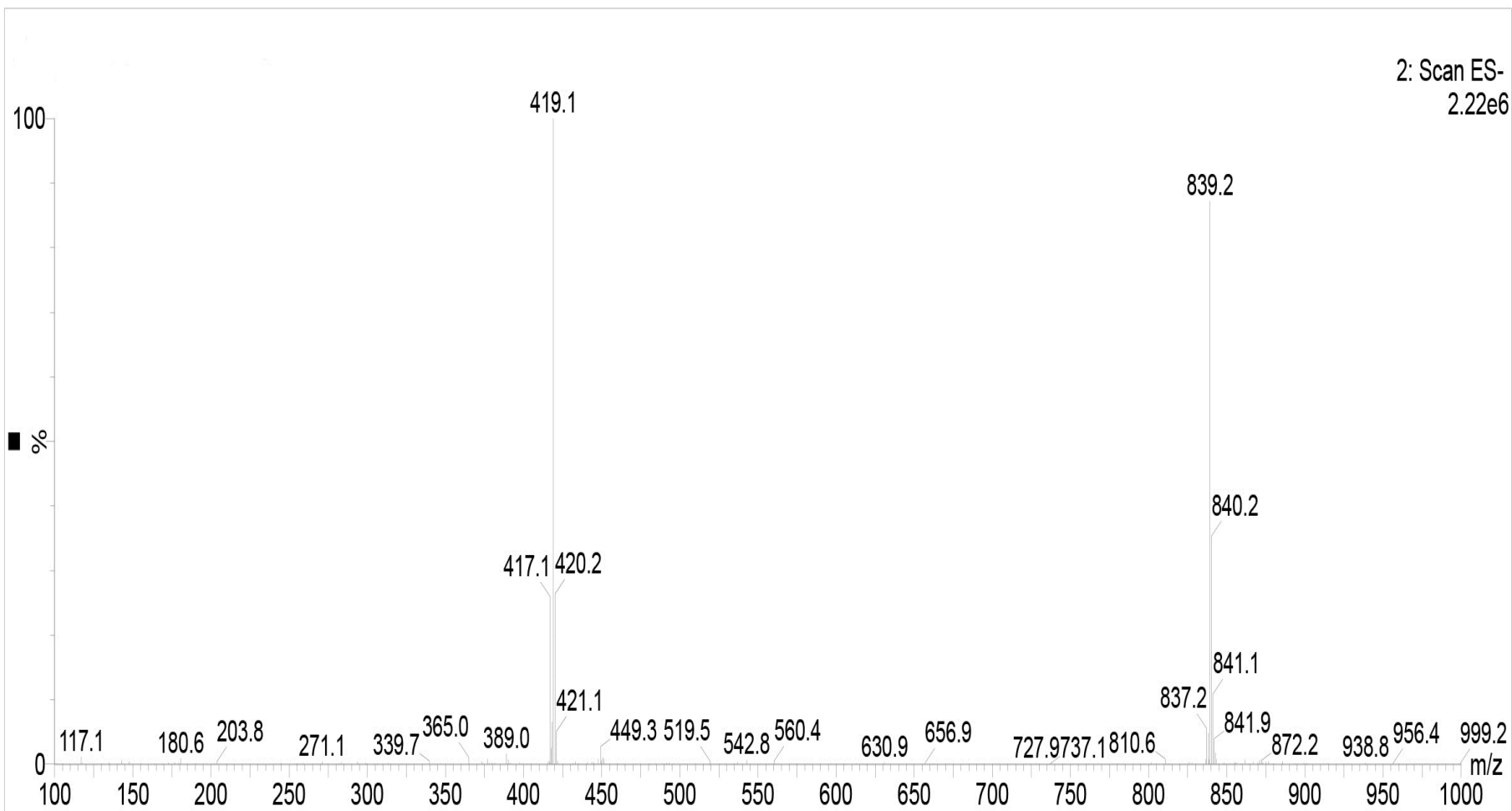
S14. ESIMS spectrum of Compound 3



S15. ¹H-NMR spectrum of Compound 4



S16. ^{13}C -NMR spectrum of Compound 4



S17. ESIMS spectrum of compound 4